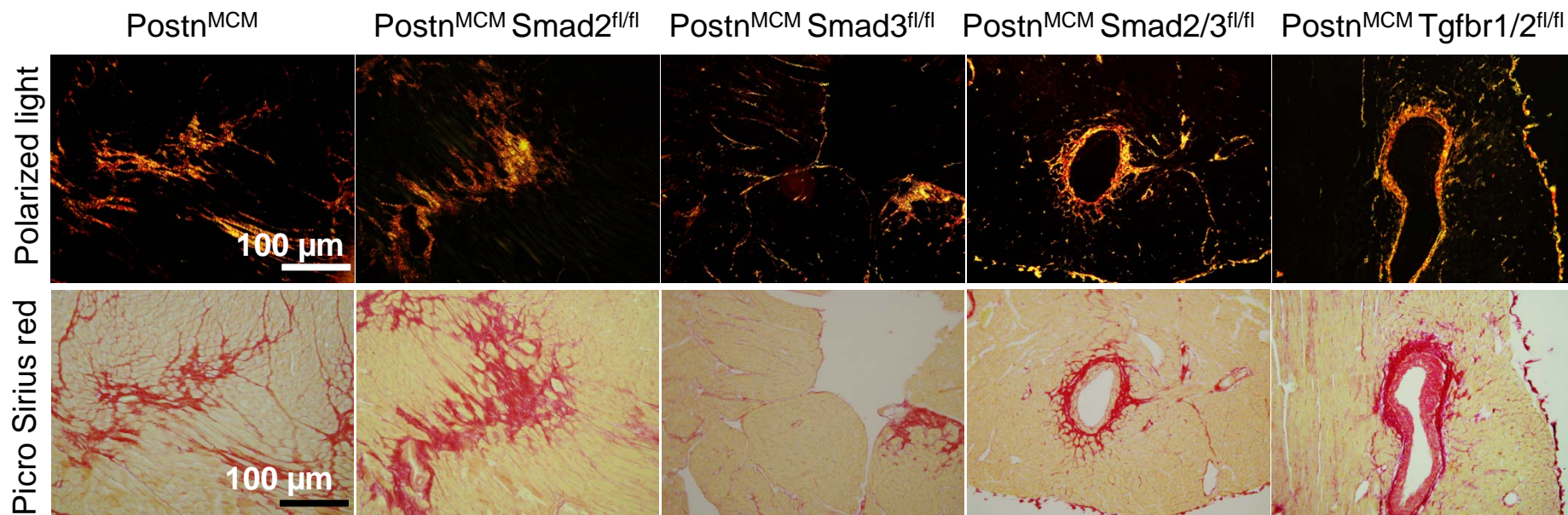**Supplemental Figure 1. Whole heart sections to accompany microscopic histological images in Figure 3 and 6. (A-D)** Masson's trichrome-stained histological whole heart images from the indicated genotypes of mice. The number of mice used in each of the experimental cohorts is discussed in the primary figures 3 and 6. Scale bar 1 mm. Fibrotic areas stain blue.

Supplemental Figure 2. Fibroblast-specific deletion of canonical TGFβ signaling does not modulate collagen maturation after TAC injury. Representative Picro-sirius red-stained histological pictures (bottom) and their corresponding polarized microscopy to show collagen complexity (top) in hearts from the indicated genotypes of mice after 12 weeks of TAC injury and continuous tamoxifen treatment. n=5 mice in each group. The data again show a reduction in cardiac fibrosis with *Postn*[MCM]-mediated deletion of *Smad3*, *Smad2/3* or *Tgfbr1/2* (Picro-sirius red staining). However, there was no apparent differences in collagen maturation in the hearts as analyzed with polarized light (orange-red birifringence) across the gentoypes. Scale bar 100 μm**.**
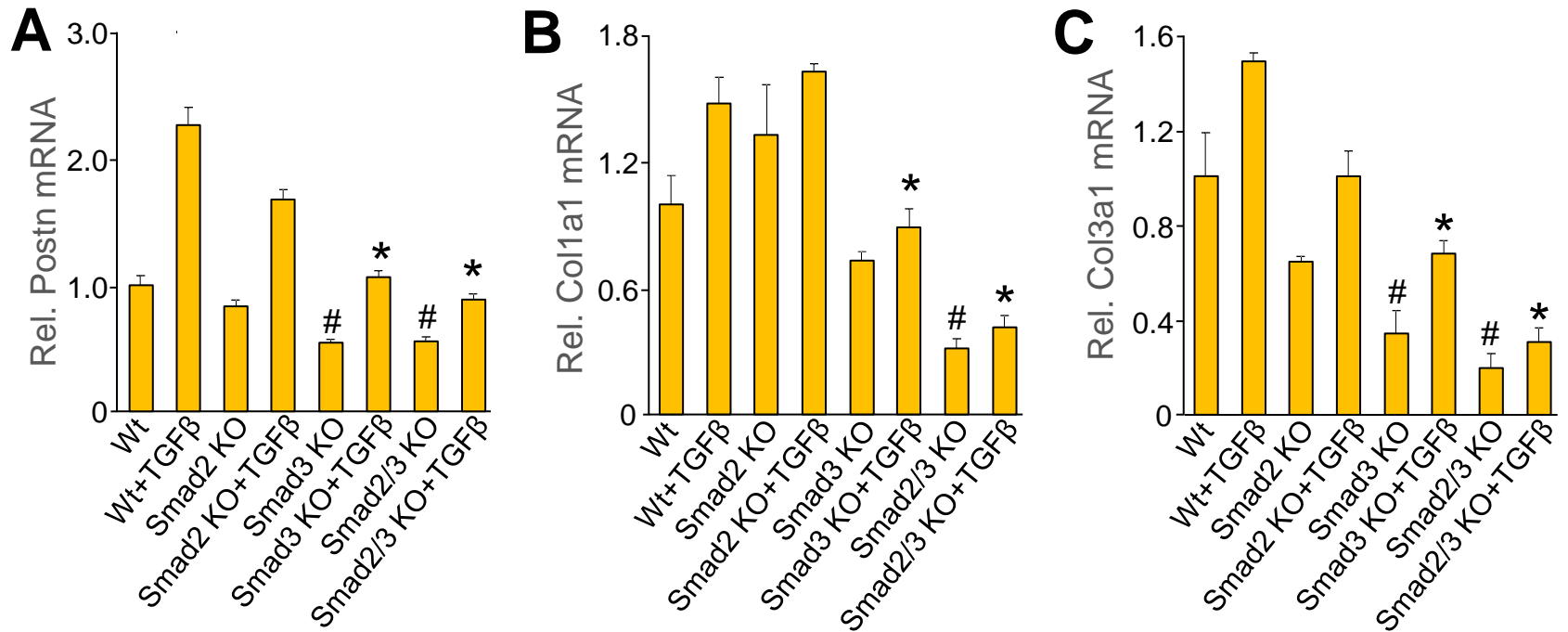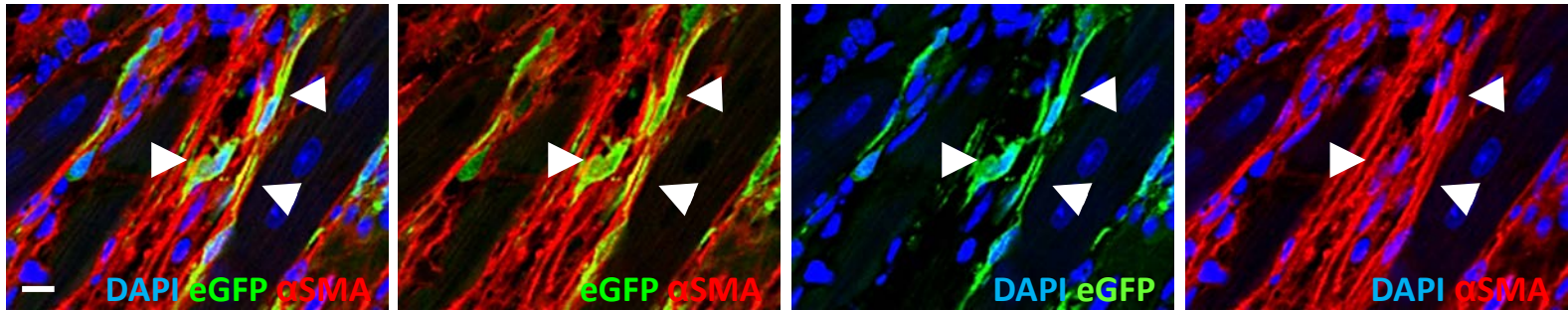
Supplemental Figure 3. Smad3 regulates ECM gene expression. (**A-C**) Adult primary heart fibroblasts were isolated from *Smad2-loxP*, *Smad3-loxP* and *Smad2/3-loxP*-targeted mice and infected with Adβgal or AdCre (KO samples). Seventy-two hrs after infection cells were treated with vehicle or 10 ng/ml of TGFβ for 24 hours. The data are real-time PCR results showing the expression levels of collagen 1a1, collagen 3a1 and periostin (Postn). n=3 separate experiments. *P<0.05 versus Wt+TGFβ; #P<0.05 versus Wt. P values represent one-way ANOVA with post-hoc Tukey HSD.
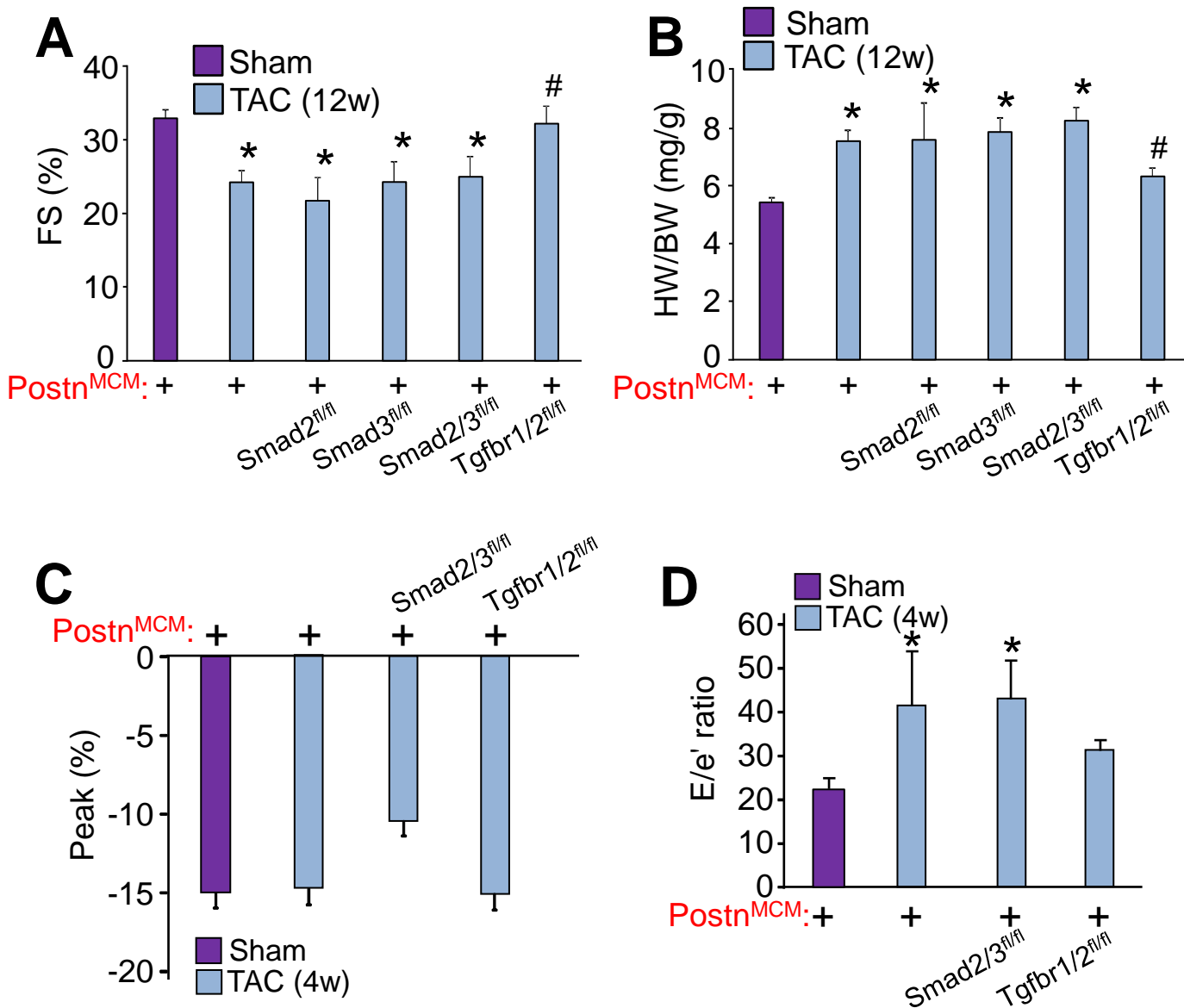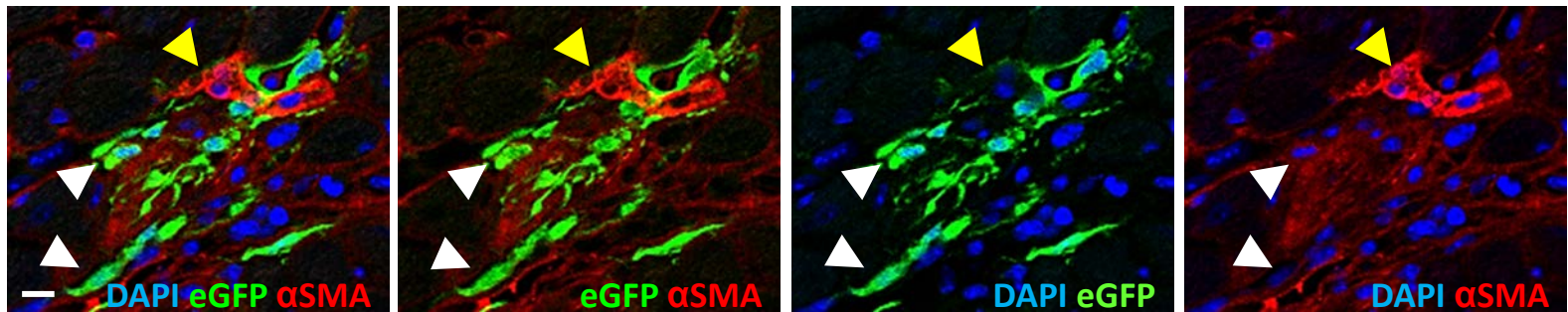
Supplemental Figure 4: Cardiac functional assessment with fibroblast-specific *Smad2/3* and *Tgfbr1/2* deletion. (**A**) Echocardiographic assessment of left ventricular fractional shortening (FS) percentage in the indicated genotypes of mice after 12 weeks of TAC injury. *P < 0.05 versus *Postn^{MCM/+}* Sham; #P<0.05 versus *Postn^{MCM}* TAC. P values were calculated with ANOVA and Tukey's post-test. (**B**) Ratios of heart-weight to body-weight (HW/BW) in mice after 12 weeks of TAC. n=7-9 in each group. *P < 0.05 versus *Postn^{MCM/+}* Sham; #P<0.05 versus *Postn^{MCM}* TAC. P values were calculated with ANOVA and Tukey's post-test. (**C**) Myocardial wall compliance assessed by echocardiographic strain (longitudinal speckle-tracking analysis) presented as a percentage of peak, 4 weeks post-TAC. The data show a trend for less wall compliance (more disease) in the *Smad2/3* double-deleted mouse hearts but not *Tgfbr1/2* double nulls. (N=3-5). (**D**) Diastolic function was assessed by tissue Doppler echocardiography as the E/e' ratio that measures mitral valve inflow maximum velocity (E-wave) to posterior wall maximum tissue Doppler velocity (e') ratio in the indicated genotypes of mice after 4 weeks of TAC (n=3-4). Statistical comparison by t-Test between sham and WT or *Smad2/3* double nulls was significant but not when compared with *Tgfbr1/2* double null. However, by one-way ANOVA the data only showed a trend and did not achieve significance. (N=3-5 mice per group).

**Supplemental Figure 5. Additional images with more fluorescent imaging channels to support Figure 4D**. Representative immunohistochemistry on cryosections from a different plane of sectioning from the heart compared with what is shown in Figure 4D. The data show eGFP-labeled (green) fibroblasts along with αSMA (red) positive cells from hearts of the indicated genotypes of mice after 4 weeks of TAC. DAPI staining shows nuclei (blue). The white arrows show eGFP+ fibroblasts, which are αSMA+ in hearts from control *Postn^MCM R26^eGFP* mice but αSMA negative in hearts from *Postn^MCM Smad2/3^fl/fl *R26^eGFP* mice. The Yellow arrow shows αSMA fibroblasts that are not eGFP+ (Representative images from n=4 hearts/mice in each of the 2 groups). Scale bars are 10 μm.

EGFP, CD31, DAPI, EdU
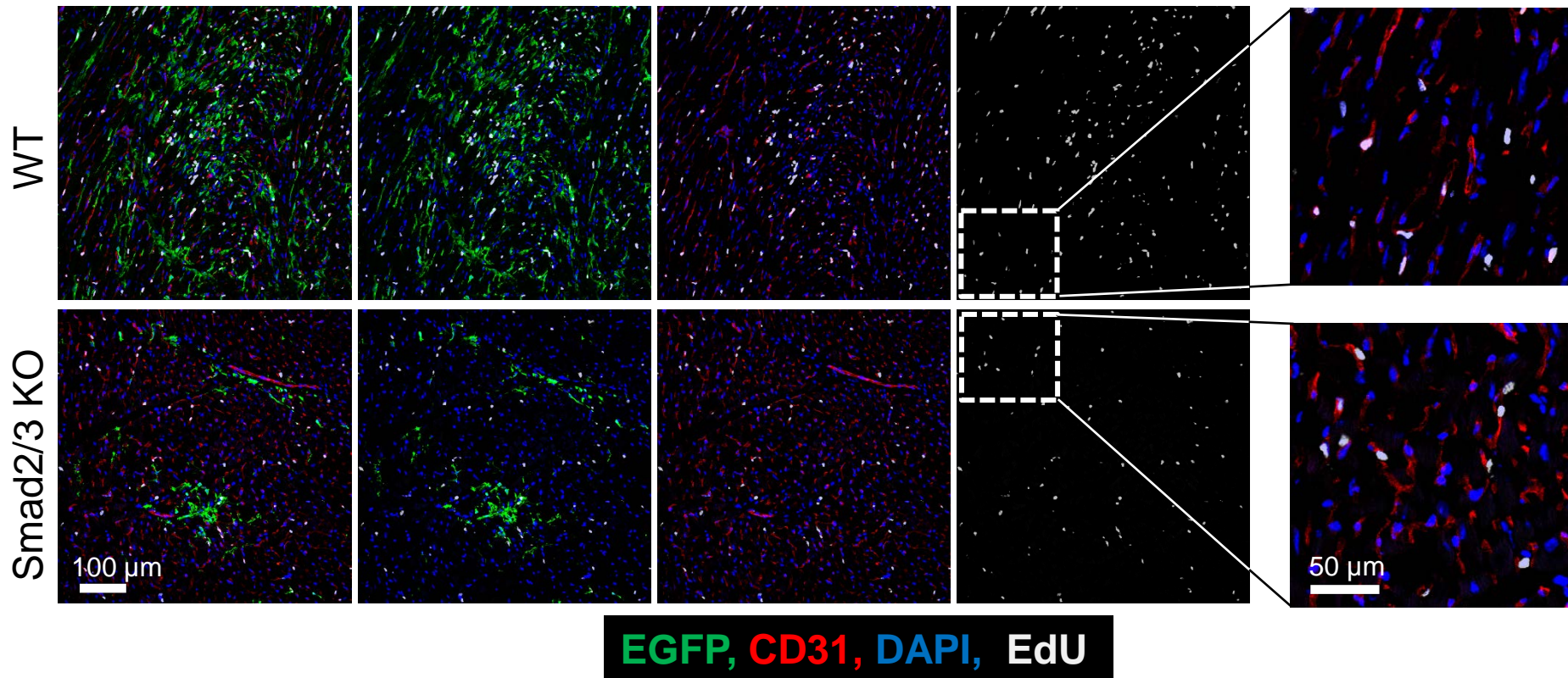
Supplemental Figure 6. Fibroblast-specific deletion of *Smad2/3* does not affect endothelial cell proliferation after TAC injury, although fibroblast proliferation is dramatically reduced. Immunohistochemical heart images from wild-type (WT) and *Smad2/3* activated fibroblast-specific knockout (KO) mice (with *Postn^MCM* allele) subjected to TAC injury as described in Figure 5D and E. Mice were injected with EdU 4 and 24 hrs before harvest. EGFP+ fibroblasts are shown in green and CD31+ endothelial cells are in red while EdU proliferation marking is in white and nuclei are blue with DAPI staining. The inset boxes correspond to high magnification images shown on the right (only the white and red channels). n=3 mice in each group. The data show that fibroblasts mostly lack EdU staining with *Smad2/3* deletion compared with WT control, although the same relative rate of endothelial cell EdU positivity between genotypes is observed. Size of the scale bars is shown in the panels.
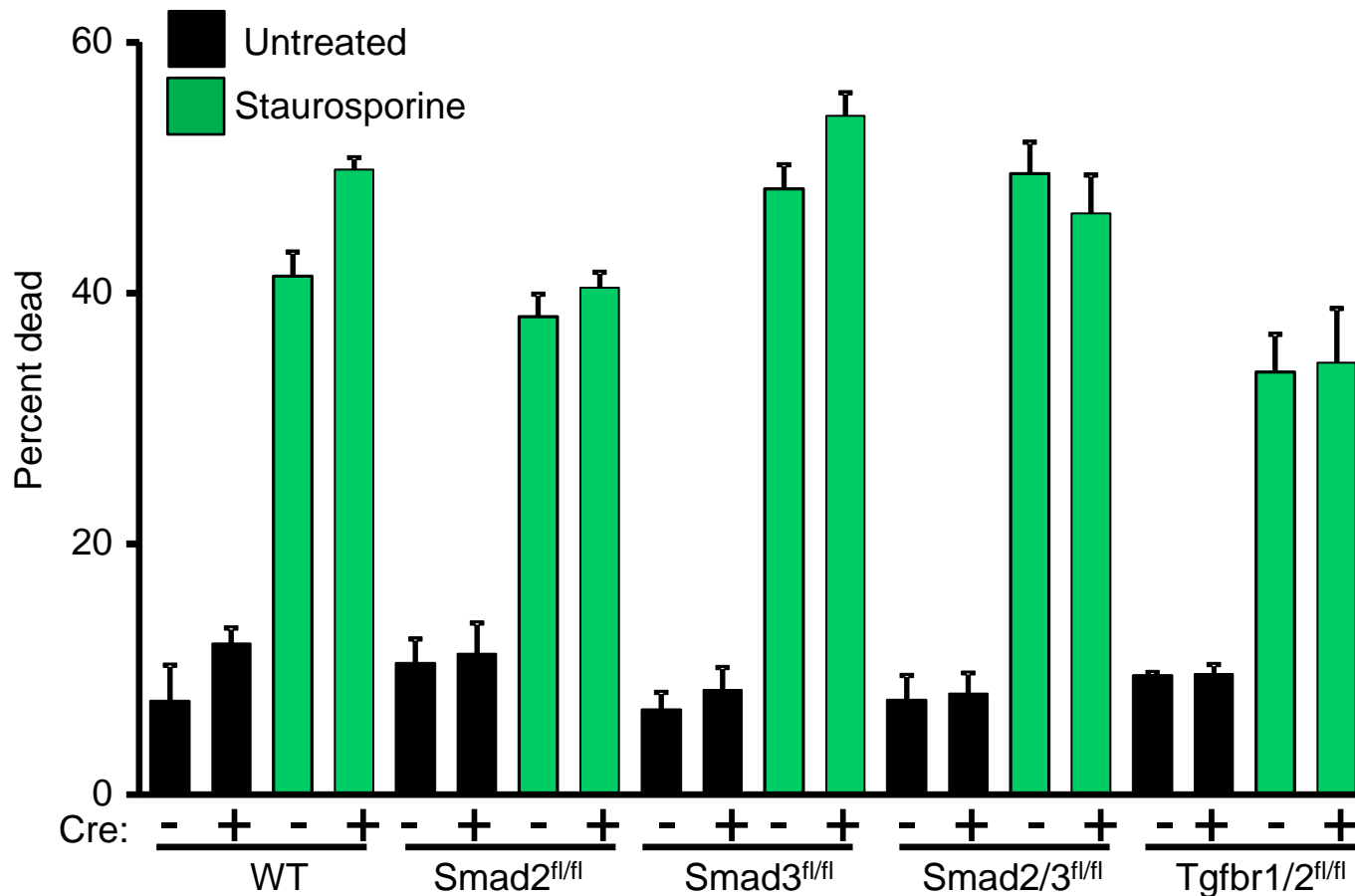
Supplemental Figure 7. Fibroblast-specific deletion of canonical TGFβ signaling does not modulate staurosprine induced apoptosis of fibroblasts. Wild-type (WT), *Smad2/3-loxP* and *Tgfbr1/2-loxP* primary skin fibroblasts were infected with Adβgal or AdCre for 96 hours and then treated with vehicle (DMSO) or 200 nM staurosporine for 36 hours. Dead cells (which have permeabilized membranes) were labeled with the Muse Count & Viability assay and quantitated using a Muse Cell Analyzer. Treatments were performed in duplicate and averaged from two independent experiments. Loss of any of the canonical TGFβ signaling genes from the genotypes of primary skin fibroblasts analyzed here had no effect on levels of staurosporine-induced apoptosis.